Pergamon

Int. J. Mach. Tools Manufact. Vol. 36, No. 11, pp. 1187–1200, 1996

0890–6955/96$15.00 + .00

PII: S0890–6955(96)00024-7

AN ANALYTICAL EVALUATION OF THE CUTTING FORCES IN SELF-PILOTING DRILLING USING THE MODEL OF SHEAR ZONE WITH PARALLEL BOUNDARIES. PART 1: THEORY

V.P. ASTAKHOV†‡ and M.O.M. OSMAN†

(*Original received* 20 *January* 1995; *in final form* 3 *February* 1996)

Abstract—The performance of a self-piloting tool is affected by its design and geometry parameters. These parameters constitute the tool-force system which directly defines quality of the machined holes, tool life and required power. This paper presents an analytical approach to describe the cutting forces in self-piloting drilling. The approach is useful at the level of tool and process design. The subject has been covered in two parts. Part one deals with the analysis of the cutting mechanics employing the shear-zone model with parallel boundaries. The analysis of the continuity condition results in better understanding of the traditional cutting model's characteristics, such as the chip compression ratio and velocity diagram. Based on this analysis and using the thermomechanical model of the work-material resistance to cutting, a cutting-force model is proposed and has been verified experimentally. Copyright © 1996 Elsevier Science Ltd

NOMENCLATURE

a	uncut chip thickness
a_1	chip thickness
b	width of cut
b_1	width of chip
c_v	specific heat capacity (at the constant volume) of workpiece material
$d\epsilon_{xy}$	infinitely small increment of angular deformation [Equation (16)]
F	tangential force on the rake surface
F_1	friction force on the flank
F_x, F_y, F_z	machine reference-system components of the cutting force
HB	Brinell hardness
h	width of shear zone
h_1, h_2, h_3	contact lengths along tool flanks
L_c	chip length
L_p	length of cut
l, l_p, l_{ef}	full length, length of plastic part, effective length of the chip–tool contact, respectively
l_1, l_2, l_3	lengths of the principal and auxiliary cutting edges
N_1, N_2, N_3	normal forces on the principal and auxiliary flanks
n	parameter in Equation (14)
$P\tau$	projection of cutting force into the shear plane
Pe	Peclet number [from Equation (22)]
q_F	yield shear stress along the effective length of chip–tool interface
R	cutting force (Fig. 6)
R_z, R_{xy}	sums of projections of the forces acting on the tool face into the z-axis and into the xy-plane, respectively
s	feed (mm/rev)
t	depth of cut (uncut chip thickness in an orthogonal model)
t_1	chip thickness in an orthogonal model
u_x (y)	displacement from Equation (15)
v	cutting speed
v_x, v_y, v_n	velocity components
v_1	chip velocity
v_2	discontinuity of the tangential velocity
v_I, v_{II}	velocities (in the shear zone) tangent to the mutual perpendicular slip lines I and II, respectively (Fig. 2)

†Department of Mechanical Engineering, Concordia University, Montreal, Quebec, Canada H3G 1M8.
‡Author to whom all correspondence should be addressed.

v_τ, $v_{1\tau}$	components of velocity [Fig. 1(b) and (c)]
w	quantity of thermal diffuseness of the workpiece material
γ	rake angle
Δt	time interval [Equation (9)]
ϵ_u	true shear strain
η	deviation angle of chip (Fig. 8)
θ	temperature in Equation (19)
θ_s	temperature in the shear zone
θ_r	temperature along the plastic part of the tool–chip contact
ζ	chip compression ratio
σ_{uts}	ultimate tensile stress of workpiece material
ϕ	shear angle
φ_I, φ_{II}	inclination angles of slip lines *I* and *II*, respectively (Fig. 2)
φ_p	cutting edge angle
φ_2, φ_3	angles of auxiliary cutting edges in Fig. 8
τ	shear stress in the deformation zone in Fig. 5
τ_y	yield shear stress of workpiece material
χ	angle of action
ω	angle between the plane of maximum shear-stress and the direction of cutting force R (Fig. 5)

1. INTRODUCTION

The machining of holes of high length to diameter ratio of high standards of size, parallelism, straightness and surface finish always presents problems. One of the most significant

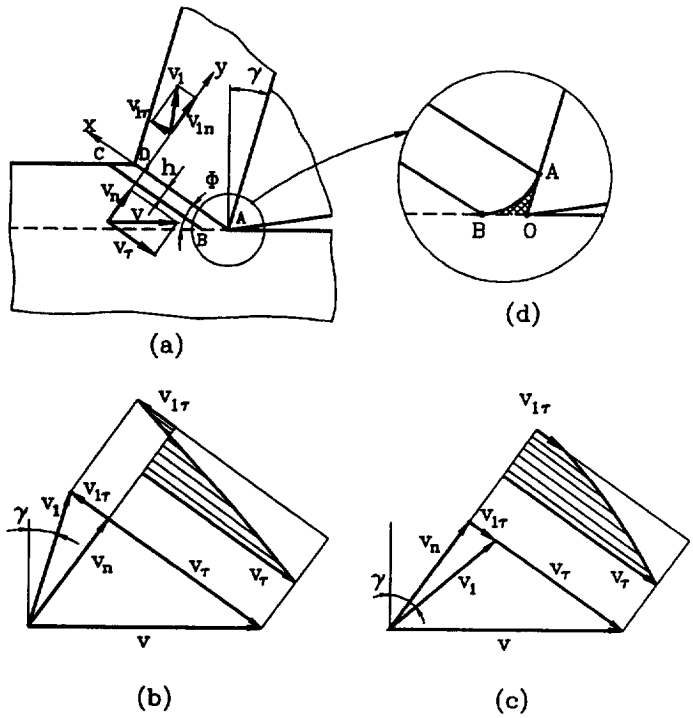

Fig. 1. Model of orthogonal cutting.

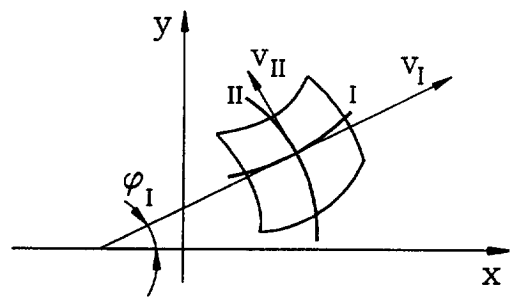

Fig. 2. Location of the tangent velocities relative to the slip lines.

technological advances made during the past 30 years to help solve these problems has been the development of the self-piloting drilling technique [1].

Originally the self-piloting tools (SPTs) served as deep-hole tools, but the method has now been adopted to even short workpieces to gain benefits of hole-axis straightness and short machining time. In mass production, a very close tolerance can be held and a reasonably high surface finish maintained. Because of the vast scale on which self-piloting drilling operations are carried out, even a slight increase in the general level of tool performance would yield important practical and economical benefits to individual firms and engineering industries.

The term "self-piloting" has grown to mean that in a particular cutting process (drilling, trepanning, boring, reaming, etc.) the resultant cutting-force projections into the radial plane (the plane perpendicular to the drill longitudinal axis) is not equal to zero and is balanced by the reactions of supporting element(s) [pad(s)] which bear against the walls of the hole being drilled. Therefore, at the start of the process a SPT guides itself into the guide bushing and then into the hole being drilled [2-4].

In order to carry out the design and optimization of SPTs, a reliable mathematical description of cutting forces for given workpiece and tool materials, cutting regime, tool geometry and design, kinematic scheme of machining, etc. is required at the stage of tool and process design.

There are two known approaches to the cutting force determination for SPT at the design stage. The first one originates from the basic relationship of the cutting mechanics and from experimental data for a given set of cutting conditions [4, 5]. The second approach employs only analytical methods to describe the cutting forces in deep-hole machining processes [6-8]. The following assumptions, which are common for both approaches, were accepted:

(1) Self-piloting drilling is considered as orthogonal cutting and a small obliquity along the cutting edge is ignored.
(2) The tool is sharp and no rubbing or ploughing occurs between the tool and workpiece.
(3) The cutting speed is high and thus the shear plane model is accepted. The stress on the shear plane is equal to the yield shear-stress for the workpiece material obtained by a tensile test on the workpiece material.
(4) There is no force acting on the tool flank, i.e. no spring-back of the machined surface occurs. As a consequence, all force-related processes which are acting on the tool wear-lands are ignored.
(5) The chip compression ratio is constant along the cutting edge. In practical terms this means that the specific cutting force is uniformly distributed along the cutting edge even though the cutting speed varies from the maximum (at the SPT periphery) to a very small value (at the SPT centre) along this edge. This makes the force calculations "insensitive" to the geometry and radial location of any of the SPT's cutters which together form the cutting edge.

As shown by the practice of tool design and by a comparison of the theoretical and experimental data, these assumptions make the cutting-force calculations very rough. The use of such models in practice is limited not only by the inaccuracy of the existing models, but also by the inability of the known models to take into consideration the specific design of tool components, their geometry and their location.

This paper presents a method for cutting forces evaluation in self-piloting drilling to be used at the design and optimization stage (without resorting to empirical equations). The method is based on the model of shear zone with parallel boundaries. The main advantage of this model is the ability to take into consideration the main components of tool design and geometry, the cutting regime and coolant supply conditions.

2. ELEMENTS OF CUTTING MECHANICS

The proposed approach involves the increased development of the shear-zone model with parallel boundaries and the analysis of the basic relationships in metal cutting. The

concept of the shear zone with parallel boundaries has been developed for many years now [9, 10]. Strong experimental evidence in support of the concept was provided by Spaans [11]. However, it was accepted that both the stress and the hydrostatic pressure are constant within the zone's limits, which evidently is in contradiction with the mechanics of materials [12].

2.1. *Analysis of the continuity condition*

A simple model of two-dimensional machining (orthogonal cutting) is shown in Fig. 1(a). The tool is a single-point tool characterized by the rake angle γ. The forces imposed on the tool create intense shearing action on the metal ahead of the tool. The metal in the chip is severely deformed on changing from an undeformed chip of thickness t to a deformed chip with thickness t_1 as a result of shear in the shear zone ABCD with parallel bounders, occurring at shear angle ϕ.

The coordinate system, illustrated in Fig. 1, is described as follows:

- the x-axis coincides with the upper boundary of the shear zone ABCD;
- the y-axis is perpendicular to the x-axis as shown in Fig. 1.

It is generally considered that the continuity condition for a state of plane strain model is [9, 10]:

$$\frac{\partial v_x}{\partial x} + \frac{\partial v_y}{\partial y} = 0 \tag{1}$$

This condition can be simplified using the fact that the upper boundary of the shear zone is a slip line. It is known that for velocities v_I and v_{II}, tangent to the mutual perpendicular slip lines I and II (Fig. 2), the Geiringer equations are valid [10]:

$$dv_I - v_{II} d\varphi_I = 0 \tag{2}$$

$$dv_{II} + v_I d\varphi_{II} = 0 \tag{3}$$

Since the upper boundary of the shear zone is a straight line then $d\varphi_I = 0$. Thus from Equation (2),

$$dv_I = 0 \Rightarrow v_I = \text{constant} \tag{4}$$

Hence, the velocity along a straight slip line is constant. This leads to

$$\frac{\partial v_x}{\partial x} = 0 \tag{5}$$

and Equation (1) becomes

$$\frac{\partial v_y}{\partial y} = 0 \Rightarrow v_y = \text{constant} \Rightarrow \text{proj.}_y v = \text{proj.}_y v_1 \Rightarrow v_n = v_{n1} \tag{6}$$

Referring to Fig. 1, Equation (6) shows that the velocity in the y-direction in the deformation zone with parallel boundaries is constant. This deduction is of major importance in the latter analysis of strains in this zone.

Since v_y=constant, it follows from Equation (3) that $dv_{II} = 0$. This in turn results in the following:

$$d\varphi_{II} = 0 \Rightarrow \varphi_{II} = \text{constant} \tag{7}$$

Therefore the second family of slip lines is a set of straight lines. Due to the orthogonality of the slip lines, the second deformation zone with parallel slip lines is attached to the straight upper-boundary.

Referring to Fig. 1, Equation (6) may be written as follows:

$$v\sin\phi = v_1\cos(\phi-\gamma) \tag{8}$$

The ratio of velocities v and v_1, or the ratio of the length of cut L_p to the chip length L_c is known as the chip compression ratio ζ [13, 14]:

$$\frac{v}{v_1} = \frac{v\Delta t}{v_1\Delta t} = \frac{L_p}{L_c} = \zeta = \frac{\cos(\phi-\gamma)}{\sin\phi} \tag{9}$$

As might be expected, this well-known equation is another form of the continuity condition which is actually the condition of contact between the chip and the deformation zone along its straight upper-boundary. Therefore Equation (9) is valid for any accepted shape of the shear zone with a straight upper-boundary.

The chip compression ratio is widely used in metal-cutting studies due to the relative simplicity of its determination [13, 14]. It should be emphasized here that the chip compression ratio approach is valid not only for conditions of two-dimensional, but also for three-dimensional machining and that the chip compression ratio does not depend on the shape of the chip cross-section. When the chip cross-section has a trapezoidal or even a triangular shape (which is common for real cutting conditions in self-piloting drilling, Fig. 3), the chip compression ratio reflects the compression of chip relative to the uncut chip thickness, i.e.

$$\zeta = \frac{a_1(z)}{a(z)} \tag{10}$$

The chip compression ratio is a non-dimensional parameter [Equation (9)] used as a scale factor for ascertaining the similarity between cutting processes. In this connection it is appropriate to mention here the following. It becomes customary to consider that, in a general case, the chip width b_1 is greater than the uncut chip width b [10, 14], thus explaining the difference between two- and three-dimensional machining. The experimental comparison of the chip width b_1 and the width of cut b has been carried out for a wide

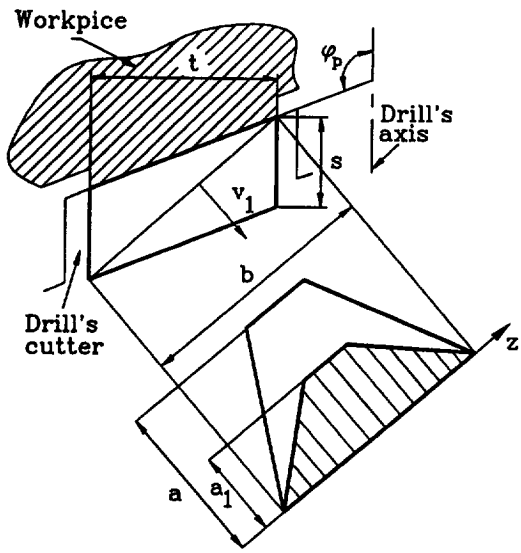

Fig. 3. Transformation of the chip shape in the direction of its sliding.

range of cutting conditions and different machining operations. A typical result of such a comparison for turning is given in Fig. 4 (cutting speed 125 m/min, workpiece material AISI 1040, 220 *HB*, tool material carbide C-6, tool geometry ISO 3001/1, 1977), cutting edge angle 45°, rake angle 5°, inclination angle 0°). It shows that the chip width b_1 is practically equal to the width of cut b when b is calculated accounting for the direction of chip sliding along the tool face, i.e.

$$b = \sqrt{t^2 + (t\cot\varphi_p + s)^2} \tag{11}$$

Here t is the depth of cut, φ_p is the cutting edge angle and s is the feed. Therefore the assumption of true plane-strain conditions in metal cutting has a reasonable justification.

2.2. *Permissible velocities, displacements and deformation in the shear zone*

According to the continuity condition [Equation (6)], the boundary conditions for the tangential and normal velocity components [Fig. 1(a)] are

$$v_x = \begin{cases} v_\tau = v\cos\phi & \text{when } y = -h \\ v_{1\tau} = -v_1\sin(\phi-\gamma) & \text{when } y = 0 \end{cases} \tag{12}$$

$$v_y = v_n = v\sin\phi$$

The component of the workpiece velocity v_τ and the component of chip velocity $v_{1\tau}$ with respect to the shear zone can have either the same [Fig. 1(b)] or opposite direction [Fig. 1(c)] depending on a particular combination of the angles ϕ and γ. The shearing process in the latter case has been widely considered [9, 10, 13, 14], while the former case requires some attention.

As one might expect from Fig. 1, the velocity components v_τ and $v_{1\tau}$ have the same direction if and only if the rake angle γ is greater than the shear angle ϕ. As such, the deformation process is quite special. Consider the interaction between the tool and the workpiece when the wedge rake angle is chosen to be very large, e.g. γ=30–45°. The reduction of the plastic-deformation rate in cutting with a large γ leads to the condition where the angle ω between the plane of maximum shear-stress and the direction of the cutting force R becomes close to 90° (Fig. 5). Such a model allows one to compare the compression of the work material by the tool face with the pressing of a wedge-shaped workpiece between a pair of flat plates inclined with a small angle relative to each other. In cutting, the role of one of the plates plays the tool face and the role of another plate plays the layer of metal being removed where the plastic deformation has not yet occurred (the conditional boundary between the plastic and elastic zone is shown in Fig. 5 as line ML). Under such conditions the main part of the work material flows in the direction of the "thick" part of wedge-shaped plastic-deformation zone, the internal layers flow much more intensively than the external layers and the deformation rate in the "thin" part of the wedge-shape plastic-deformation zone is much higher than in the "thick" part [15].

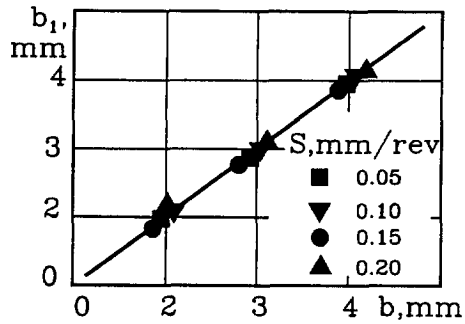

Fig. 4. Experimental comparison of the uncut chip width b and chip width b_1.

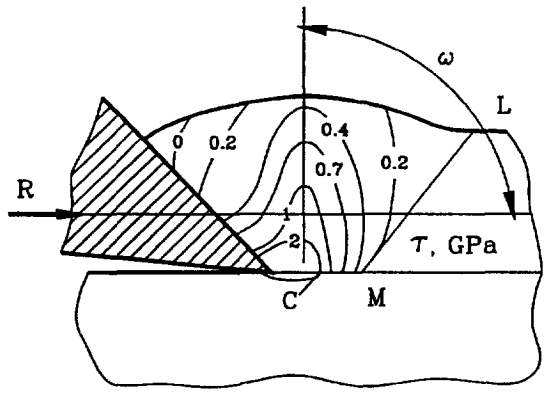

Fig. 5. Model for cutting with a very high rake angle.

The finite element analysis of the state of stress [16] conducted for the model conditions (γ=30°, v=70 m/min, t=2 mm, workpiece material=steel AISI 1040, as rolled) confirms (Fig. 5) the described chip formation process under these conditions. The continuous uniform-strength chip is formed. The wedge-shaped grains can be clearly seen via microphotography (Fig. 6) where a higher deformation rate is observed at the "thin" part of grains.

The difference between the velocities v_τ and $v_{1\tau}$ defines the discontinuity v_2 of the tangential velocity v_x with respect to the shear zone:

$$v_2 = v_\tau - v_{1\tau} \tag{13}$$

$$v_2 = v\cos\phi + v_1\sin(\phi-\gamma) = v\frac{\cos\gamma}{\cos(\phi-\gamma)}$$

The discontinuity v_2 of the tangential velocity v_x during the transformation of a deformed fragment from the workpiece into the chip should be considered as an inherent feature of the shear plane model phenomenon in the cutting process. In practice, the shear zone always has a certain width h, along which the continuous transformation of the velocity v_x from v_τ to $v_{1\tau}$ takes place. Thus the change may be approximated by the suitable continuous transition curve justifying the boundary conditions [Equation (12), Fig. 1(b) and (c)]. Since the slip lines are straight lines, the velocity v_x depends on the y-coordinate only. The law governing this dependence is unknown. However, using the experimental data and existing experience [9–14, 17–20], the curve $v_x(y)$ can be approximated by the following analytical function:

$$v_x(y) = v_\tau - v_2\left|\frac{y}{h}\right|^n \tag{14}$$

Here n is a parameter (power) characterizing the non-uniform distribution of the tangential velocity in the shear zone. A detailed analysis of a large number of works dealing with the study of deformation zone in metal cutting shows that the lower limit n=4 corresponds

Fig. 6. Microphotograph of the chip obtained in cutting with a very high rake angle.

to the machining of copper at a low cutting speed (4 m/min) [14], and that the the upper limit n=10 corresponds to the machining of high carbon steels at high cutting speeds (up to 220 m/min) [21]. Therefore a reasonable value of n=6–8 may be accepted for practical cutting conditions.

Having found the velocities, it is possible to find the displacement $u_x(y)$ as

$$u_x(y) = \int_0^{y/v_n} v_x\left(\frac{y}{v_n}\right) \mathrm{d}\left(\frac{y}{v_n}\right) = \frac{v_\tau}{v_n} - \frac{v_2}{v_n}\frac{h}{n+1}\left(\frac{y}{h}\right)^{n+1} \tag{15}$$

The function $u_x(y)$ defines the trajectory of an element through its successive deformation stages, i.e. $u_x(y)$ is the equation for the streamlines in the deformation zone restricted by the parallel boundaries. Using this function, the corresponding acceleration, strain and strain-rate histories can then be computed [10, 22, 23]. For example, using the known fact that the streamlines in the deformation zone are equidistant [10, 11, 19], the shape and dimensions of the built-up edge [Fig. 1(d)] can be defined as functions of the cutting parameters.

To calculate the true shear-strain, consider the displacements in the deformation zone with parallel boundaries [Fig. 1(a)]. According to the theory of deformation [12], an infinitely small increment of angular deformation can be defined as the sum of partial strain increments along the x- and y-axes. In the coordinate system used in Fig. 1, an infinitely small increment of angular deformation is

$$\mathrm{d}\epsilon_{xy} = \frac{\partial}{\partial y}(\mathrm{d}u_x) = \frac{\mathrm{d}}{\mathrm{dy}}[\mathrm{d}u_x(y)] = \frac{n}{h}\frac{v_2}{v_n}\left(\frac{y}{h}\right)^{n-1}\mathrm{dy} \tag{16}$$

The true shear strain ϵ_u in the chip formation zone is defined by integration of Equation (16):

$$\epsilon_u(y) = \int_0^y \frac{n}{h}\frac{v_2}{v_n}\left(\frac{h}{y}\right)^{n-1}\mathrm{dy} = \frac{v_2}{v_n}\left(\frac{y}{h}\right)^n \tag{17}$$

The expression for the final true shear strain ϵ_u=$\epsilon_u(h)$ when y=h coincides with the equation commonly used in cutting theory for the shear strain:

$$\epsilon_u(h) = \frac{v_2}{v_n} = \frac{\cos\gamma}{\cos(\phi-\gamma)\sin\phi} \tag{18}$$

Following from the derivation of Equation (18), the final true shear-strain $\epsilon_u(h)$ (when the deformation of work material is considered in the zone with parallel boundaries) does not depend upon the zone's width h and the power n of non-uniform distribution of strain, but is entirely defined by the values of the discontinuity v_2 and the normal velocity v_n. Since $\epsilon_u(h)$ and n are found to be independent, Equation (18) is also valid for the single shear-plane model, which now may be considered as a limiting case of the model with parallel boundaries when $n\to\infty$.

3. CUTTING FORCES

The relationships obtained above make it possible to consider the cutting forces.

3.1. *Thermomechanical model of the workpiece-material resistance to cutting*

The thermomechanical model of the workpiece material resistance to cutting was first proposed by Kushner [24]. Specifically, by studying a wide range of engineering steels, he proposed to calculate the yield shear-strength of the workpiece material as follows:

$$\frac{\tau_y}{\sigma_{uts}} = \frac{1}{(1 + 0.5 \cdot 10^{-3}\theta)} \tag{19}$$

Here τ_y is the yield shear strength (MPa), σ_{uts} is the ultimate tensile strength (MPa) of the workpiece material and θ is the temperature (°C).

According to the thermomechanical model, the yield shear-stress of the workpiece material is temperature-dependent and decreases at a defined rate as temperature increases. Summarizing the experimental data for a wide range of the workpiece materials, Fig. 7 shows that this rate is constant [24].

An analysis of the works studying temperatures in metal cutting [10, 22, 24] reveals that the average temperature in the shear zone θ_s (°C) can be defined as

$$\theta_s = \frac{\sigma_{uts}}{c_v} \epsilon_u \tag{20}$$

where c_v is the specific heat capacity (at constant volume) of the workpiece material [MJ (K/m^3)]. The average temperature along the plastic part of the tool–chip interface θ_r (°C) can be defined as [24]

$$\theta_r = 79\left(\frac{\tau_y}{100c_v}\right)^{0.8} (Pe)^{0.4}\left(\frac{l_p}{a}\frac{1}{\zeta}\right)^{0.4} \tag{21}$$

Here l_p is the length of the plastic part of the tool–chip contact m and Pe is the Peclet number:

$$Pe = \frac{va}{w} \tag{22}$$

where: v is the velocity of a heat source (the cutting speed) (m/s); a is the uncut chip thickness (m); and w is quantity of thermal diffuseness of the workpiece material (m^2/s).

3.2. *Cutting forces*

Theoretical determination of the cutting force is one of the main concerns in metal cutting. Figure 8 shows the physical and machine reference systems components of the cutting force acting on the drill's cutting element. The machine reference-system components F_x, F_y and F_z include the sum of the projections of the forces acting on the cutting element's rake and flank into the machine reference-system x-, y- and z-axes:

$$F_x = R_{xy}\sin(\varphi_p - \eta) + N_1\sin\varphi_p - N_2\sin\varphi_2 + N_3\sin\varphi_3 \tag{23}$$

$$F_z = R_z + F_1 \tag{24}$$

$$F_y = R_{xy}\cos(\varphi_p - \eta) + N_1\cos\varphi_p - N_2\cos\varphi_2 + N_3\cos\varphi_3 \tag{25}$$

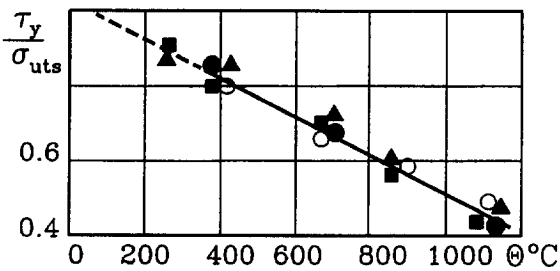

Fig. 7. Effect of temperature θ on the ratio τ_y/σ_{uts}: ▲, AISI 1045; ■, AISI 4140; ○, AISI 1065; ⊕, 8% Ni, 18% Cr steel [24].

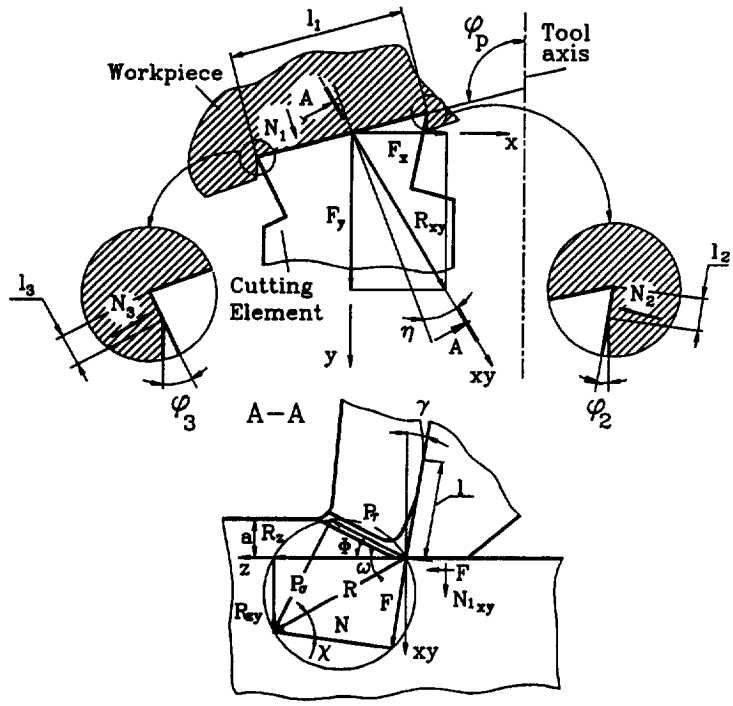

Fig. 8. Physical and machine reference-system components of the cutting force acting on the drill's cutting element.

Here R_z and R_{xy} are the sums of projections of the forces acting on the cutting element face into the z-axis and the xy-plane, respectively. F_1 is the friction force acting on the flank, and N_1, N_2 and N_3 are the normal forces on the main and auxiliary flanks, respectively. η is the angle of deviation of the chip sliding direction from the normal to the projection of the main cutting edge into the xy-plane. Using the known approach [14], this angle can be defined as

$$\eta = (\vartheta_2 - \vartheta_3) - \arctan(\tan\gamma \sin(\vartheta_2 - \vartheta_3)),\ \vartheta_i = 0.5\arcsin\left(\frac{l_i}{l_1}(\sin\varphi_p - \sin\varphi_i)\right),\ i = 2,3 \tag{26}$$

Here l_1, l_2 and l_3 are the lengths of the principal and auxiliary cutting edges (Fig. 6). Since in the design practice of SPT the ratios l_2/l_1, l_3/l_1 and angles φ_2, φ_3 are very small, the deviation angle can be neglected (except in the special cases of the cutting element location).

The projection of the cutting force R into the shear plane, P_τ (Fig. 6) is usually used for the calculation of forces acting on the tool rake surface. To calculate this force component it is necessary to know the yield shear strength τ_y of the workpiece material, the chip compression ratio ζ and the uncut chip thickness a and width b:

$$P_\tau = \tau_y \frac{ab}{\sin\phi} = \sigma_{uts} st \frac{\tau_y}{\sigma_{uts}} \frac{1}{\sin\phi} \tag{27}$$

Substituting Equations (19) and (20) into Equation (27) gives

$$P_\tau = \sigma_{uts} st \left(\frac{1}{1 + 0.5\cdot 10^{-3} \frac{\sigma_{uts}}{c_v} \frac{\zeta + \frac{1}{\zeta} - 2\sin\gamma}{\cos\gamma}} \right) \frac{1}{\arctan\frac{\cos\gamma}{\zeta - \sin\gamma}} \tag{28}$$

Since the cutting force R cannot be defined by only one of its projections, the determination of the angle of action, χ (Fig. 8), or the angle of friction using additional assumptions has been proposed [10, 14, 23]. The determination of these angles is one of the weakest aspects of the existing metal cutting theories. It can be avoided by computing the tangential force acting on the tool face:

$$F = q_F b l_{ef} = \sigma_{uts} s t \frac{q_F}{\sigma_{uts}} \frac{l_{ef}}{a} \tag{29}$$

Here q_F is the yield shear-stress along the effective length l_{ef} of the chip–tool interface and $q_F = \tau_y$ [Equation (19)] when $\theta = \theta_r$ [Equation (21)], hence

$$\frac{q_F}{\sigma_{uts}} = \frac{\tau_y}{\sigma_{uts}} \left(1 - 39.5 \cdot 10^{-3} \left(\frac{\tau_y}{\sigma_{uts}} \frac{\sigma_{uts}}{100 c_v}\right)^{0.8} \left(Pe \frac{l_p}{a} \frac{1}{\zeta}\right)^{0.4}\right) \tag{30}$$

where

$$\frac{\tau_y}{\sigma_{uts}} = \frac{1}{1 + 0.5 \cdot 10^{-3} \dfrac{\sigma_{uts}}{c_v} \dfrac{\zeta + \dfrac{1}{\zeta} - 2\sin\gamma}{\cos\gamma}} \tag{31}$$

Experiments show [10, 14] that the following relations exist between the full length of contact l, the effective length of contact l_{ef} and the length of plastic part of the tool–chip contact l_p:

$$l_p = 0.75 l_{ef} = 0.5 l \tag{32}$$

where

$$l = a\zeta^{1.5} \tag{33}$$

The component R_z is defined through the known components P_τ and F as follows:

$$\begin{aligned} R_z &= F\sin\gamma + N\cos\gamma \\ &= F\sin\gamma + \left(F\tan(\phi - \gamma) + \frac{P_\tau}{\cos(\phi - \gamma)}\right)\cos\gamma \\ &= F \frac{\sin\phi}{\cos(\phi - \gamma)} + P_\tau \frac{\cos\gamma}{\cos(\phi - \gamma)} \end{aligned} \tag{34}$$

Similarly,

$$R_{xy} = F \frac{\sin\phi}{\cos(\phi - \gamma)} - P_\tau \frac{\cos\gamma}{\cos(\phi - \gamma)} \tag{35}$$

The cutting forces on the flanks can be defined using the following known approach [14]:

$$N_1 = \frac{HB}{3} \frac{t}{\sin\varphi_p} h_1$$

$$N_2 = \frac{HB}{3} \frac{s}{\sin\varphi_2} h_2$$

$$N_3 = \frac{HB}{3}\frac{s}{\sin\varphi_3}h_3$$

$$F_1 = 0.2HB\left(\frac{t}{\sin\varphi_p} + s\right) \tag{36}$$

Here HB is the Brinell hardness of the workpiece material, and h_1, h_2 and h_3 are the contact lengths along the corresponding flanks. Usually h_1=(0.3–0.6) mm, h_2 and h_3=(0.2–0.3) mm. The accuracy of the force calculation depends upon the precision of the determination of such parameters as the chip compression ratio and the value of relative contact length between the tool and chip (l_1/a).

In order to assess the accuracy of the above proposed prediction of the cutting forces, a series of experiments were conducted. A special simulator comprising a self-piloting drill with an indexable cutting insert was used [4]. The conditions of the tests were selected as follows:

(1) Workpiece material—AISI 4140, σ_{uts}=845 MPa, σ_{uts}/c_v=167, c_v=5.0 MJ (K/m^3), w=8.00·10^{-6} m^2/s. The composition, the elements limits and the deoxidation practice were chosen to be in agreement with the requirements of standard ANSI/ASME B94.55M (1985). The test bars, after being cut to length (40 mm diameter, 50 mm length) were normalized to a Brinell hardness of 200 HB. The hardness of the work material was determined over the complete cross-section of the end of each test bar and cutting tests were conducted only on the bars where the hardness was within the limits±10%. Special parameters such as the microstructure, grain size, inclusions count, etc. were checked using quantitative metallography.
(2) Cutting tool—a simulator of a self-piloting drill with external chip removal of 40 mm diameter has been used. The tool material was carbide C-6. The geometry parameters of the cutting insert were chosen according to recommendations in Ref. [1].
(3) Cutting fluid—"Shell Garia H" cutting fluid with the flow rate of 0.7·10^{-4} m^3/s was used for the experiments [25, 26].
(4) Dynamometer—the dynamometer design (Kistler 9271A) and its static and dynamic calibration have been presented in detail in earlier work [27, 28].

The cutting forces, chip compression ratio and effective length of tool–chip contact were measured experimentally using the methodology presented in Ref. [14].

Table 1 shows the calculated [using Equation (25) for F_z and Equation (35) for R_{xy}] and experimental results. As can be seen from this table the accuracy of the proposed model for force calculation is within the limits of 10–15%.

4. CONCLUSIONS

The shear-zone model with parallel boundaries has been chosen as a model for the analysis of the mechanics of cutting and cutting-force determination. This analysis leads to the following conclusions:

(1) Two families of straight-slip lines constitute the deformation zone in metal cutting;

Table 1. Comparison of the calculated and experimental values of the cutting forces

γ (°)	S (mm/rev)	t (mm)	v (m/s)	10^3va (m^2/s)	ζ	l/a	F_z, N		R_{xy}, N	
							Calculated	Experimental	Calculated	Experimental
+10	0.26	4	1.2	0.30	2.1	3.27	2392	2187	898	994
+5	0.22	4	1.2	0.26	2.3	3.81	2089	2339	1222	1368
0	0.18	4	1.2	0.20	2.5	4.31	2307	2194	1490	1437
0	0.14	4	1.8	0.24	2.8	4.88	1881	1678	1046	1112
−5	0.12	4	1.8	0.21	3.5	6.81	1557	1732	1282	1347
−10	0.10	4	1.8	0.17	4.5	9.84	1715	1954	1385	1489

one family is parallel and another is perpendicular to the straight upper boundary of this zone.

(2) The well-known equation for the chip compression ratio is another form of the continuity condition. This equation is valid for any assumed shape of shear zone with a straight upper boundary. The chip width, when calculated in the direction of chip sliding, is equal to the width of cut. This fact provides reasonable justification for the consideration of true plane strain conditions in metal cutting.

(3) The discontinuity of the tangential velocity (the component of the cutting speed which is parallel to the boundary of the shear zone) during the transformation of a deformed fragment from the workpiece into the chip is an attribute of the shear plane model phenomenon in the cutting process. In practice, the shear zone always has a certain width along which the continuous transformation of this velocity takes place. Therefore the acceleration, strain and strain-rate in the shear zone with parallel boundaries are not uniformly distributed as considered before. The final true shear strain depends upon neither the zone's width nor the power of non-uniform distribution of strain, but is entirely defined by the values of the discontinuity of the tangential and normal velocities. Therefore the shear-plane approximation, considered as a limiting case of the shear zone model with parallel boundaries, is a good model for a real cutting process when deformation in the metal cutting is of prime concern.

(4) The thermomechanical model of the work-material resistance to cutting defines the ratio of the yield shear stress (in the shear zone and in the plastic zone on the tool rake) to the ultimate tensile stress as a linear function of cutting temperature. Based on this, a model for the cutting force components is suggested. To avoid the determination of the angle of action or friction angle, the computation of the tangential force acting on the tool face is proposed. The predicted results of cutting force have been compared with the experimental data. The agreement is fairly good. The derived equations for the prediction of cutting forces acting on a drill's cutting element are suitable for the application of the force calculations in the design of SPT.

Acknowledgements—The financial support of the Natural Science and Engineering Research Council of Canada is gratefully acknowledged. We would like also to express our sincere gratitude to the unknown reviewers of the paper for providing constructive criticism toward the final improvement of the manuscript.

REFERENCES

[1] F.S. Bloch *et al.*, *Gundrilling, Trepanning and Deep-Hole Machining*. ASTME (1968).
[2] V. P. Astakhov, A. A. Ajrikjan and G. M. Petrosjan, Pad forces in self-piloting drilling and their experimental determination, *UKRNIINTI* **1209**, 10 (1979).
[3] B.J. Griffiths, Deep-hole drilling process and surface integrity. *2nd Int. Conf. on Deep-Hole Drilling and Boreing*, Brunel University, London (1979).
[4] V. P. Astakhov, V. V. Galitsky and M. O. M. Osman, An investigation of the static stability in self-piloting drilling, *Int. J. Prod. Res.* **33**(6), 1617 (1995).
[5] B. J. Griffiths, Modelling complex force systems. Part 1: The cutting and pad forces in deep drilling, *Trans. ASME. J. Engng Ind.* **115**, 169 (1993).
[6] S. Chandrashekhar, M. O. M. Osman and T. S. Sankar, An analytical time domain evaluation of the cutting forces in BTA deep-hole machining using the thin shear plane model, *Int. J. Prod. Res* **22**(4), 697 (1984).
[7] V. N. Latinovic and M. O. M. Osman, Optimal design of BTA deep-hole cutting tools with staggered cutters, *Int. J. Prod. Res.* **27**(1), 153 (1989).
[8] V. N. Latinovic, R. Blakely and M. O. M. Osman, Optimal design of multi-edge cutting tools for BTA deep hole machining, *Trans. ASME. J. Engng Ind.* **101**, 281 (1979).
[9] D. Kececioglu, Shear-zone size, compressive stress, and shear strain in metal cutting and their effects on mean shear-flow stress, *Trans. ASME. J. Engng Ind.* **81**, 79 (1960).
[10] P.L.B. Oxley, *Mechanics of Machining: An Analytical Approach to Assessing Machinability*. Wiley, New York (1989).
[11] C. Spaans, A treatise of the streamlines and the stress, strain, and strain rate distributions, and on stability in the primary shear zone in metal cutting, *Trans. ASME. J. Engng Ind.* **93**, 690 (1972).
[12] G.E. Dieter, *Mechanical Metallurgy*, 3rd edn. McGraw-Hill, New York (1986).
[13] I.I. Timme, *On the Resistance of Metals and Wood to Cutting* (in Russian). Dermacov, St Petersburg (1880).
[14] N.N. Zorev, *Metal Cutting Mechanics*. Pergamon, Oxford (1966).
[15] R.W. Hertzberg, *Deformation and Fracture Mechanics of Engineering Materials*, 3rd edn. Wiley, New York (1989).
[16] V. P. Astakhov, Finite element modelling of orthogonal metal cutting, *Ukrniinti* **1246**, 26 (1992).
[17] E.M. Trent, *Metal Cutting*. Butterworth-Heinemann, London (1991).

[18] R. F. Scrutton, The geometry of the shear zone in metal cutting, *Trans. ASME. J. Engng Ind.* **89**, 420 (1968).
[19] J. H. L. The, The quadratic curve and the trajectory in the shear zone in metal cutting, *Trans. ASME. J. Engng Ind.* **August**, 1105 (1975).
[20] S. Kobayashi and E. G. Tomsen, Some observations on the shearing process in metal cutting, *Trans. ASME. J. Engng Ind.* **August**, 251 (1959).
[21] D. Lee, The effect of cutting speed on chip formation under orthogonal machining, *Trans. ASME. J. Engng Ind.* **107**, 55 (1985).
[22] G. Boothroyd and W.A. Knight, *Fundaments of Machining and Machine Tools*, 2nd edn. Dekker, New York (1989).
[23] M. E. Merchant, Mechanics of the metal cutting process, *J. appl. Phys.* **16**, 267 (1945).
[24] V.S. Kushner, *Thermomechanical Approach in Metal Cutting* (in Russian). Irkutsk University Press, Irkutsk (1982).
[25] V. P. Astakhov, P. S. Subramanya and M. O. M. Osman, An investigation of the cutting fluid flow in self-piloting drills, *Int. J. Mach. Tools Manufact.* **35**(4), 547 (1995).
[26] V. P. Astakhov, P. S. Subramanya and M. O. M. Osman, Theoretical and experimental investigations of coolant flow in inlet channels of the BTA and ejector drills, *J. Engng Manufact. Part B Proc. I. Mech. E.* **209**, 211 (1995).
[27] S. Chandrashekhar, M. O. M. Osman and T. S. Sankar, An experimental investigation for the stochastic modelling of the resultant force system in BTA deep hole machining, *Int. J. Prod. Res.* **23**, 65 (1985).
[28] V. P. Astakhov, A methodology for the experimental force determination in self-piloting drilling, *Metall. Stanky* **43**, 40 (1994).